

Onset of wave fronts in a discrete bistable medium

Diego Pazó* and Vicente Pérez-Muñuzuri

Grupo de Física non Lineal, Facultade de Física, Universidade de Santiago de Compostela, 15706 Santiago de Compostela, Spain

(Received 6 March 2001; published 26 November 2001)

The transition from a standing front to a traveling front is studied in an array of symmetric bistable coupled oscillators. The mechanism leading to propagation may be understood in the context of a *gluing bifurcation* involving a pair of homoclinic loops. The velocity of the front shows a logarithmic dependence with the coupling strength according to this mechanism.

DOI: 10.1103/PhysRevE.64.065203

PACS number(s): 05.45.Pq, 42.65.-k, 45.05.+x, 87.10.+e

Pattern formation has become one of the most active areas of research [1]. The development of patterns can be attributed to the combination of diffusion and local nonlinear dynamics. Interfacial patterns can be distinguished due to the fronts that separate domains of different uniform or quasiuniform states.

One of the main categories in the reaction-diffusion systems corresponds to those whose local dynamics possesses two stable states: two fixed points, one fixed point and a cycle, etc. Here we focus on the case where two stable steady states coexist. Bistability is a simple phenomenon that appears in a great variety of contexts. Particularly important examples are found in optics [2], chemical systems [3], and biology [4–6].

Front propagation is an important mechanism for pattern formation in continuous and discrete systems. Phenomena such as crystallographic pinning and lattice anisotropy occur naturally in spatially discrete material models. In biology, examples of applications of spatially discrete models include the bidomain model for cardiac tissue (defibrillation), tissue filtration, gas exchange in lungs, and calcium waves. So far, most attention has been devoted to bistable nonsymmetric systems where the domain corresponding to the most stable state advances through the less stable one. Discrete bistable systems have been studied in this context, so propagation succeeds above a critical coupling ($D > D_{th}$). In particular, the propagation failure phenomenon [7–10] has been widely considered. However, one important fact is that symmetry does not preclude front propagation in nongradient systems. For example, Hagberg and Meron [11] have shown for the continuous FitzHugh-Nagumo model that wave propagation may be initiated through a symmetry breaking mechanism; a pitchfork bifurcation.

In this Rapid Communication, we show a transition *standing* \rightarrow *oscillating* \rightarrow *traveling* front in an array of *symmetric multivariable* bistable units. This transition seems to be exclusive for a discrete medium.

As starting point, we consider a one-dimensional array consisting of bidirectionally coupled identical units,

$$\dot{\mathbf{r}}_j = f(\mathbf{r}_j) + \frac{D}{2} \Gamma (\mathbf{r}_{j+1} + \mathbf{r}_{j-1} - 2\mathbf{r}_j), \quad (1)$$

where $\mathbf{r}_j \in R^n$. D is the coupling parameter and Γ is the coupling matrix. Although the case $n=1$ has been widely

studied [5,10,12,13], multivariable cells ($n > 1$) may show interesting phenomena, like the scenario leading to front propagation described below.

In our case, we deal with the well-known Lorenz oscillator [14] as a unit cell. In order to be the most general as possible, two kinds of coupling have been considered here, such as (i) the off-diagonal case ($\Gamma = \gamma_{kl} = \delta_{k1} \delta_{l2}$) and (ii) the on-diagonal case ($\Gamma = \gamma_{kl} = \delta_{k2} \delta_{l2}$),

$$\begin{aligned} \dot{x}_j &= \sigma(y_j - x_j) + \frac{D^a}{2}(y_{j+1} + y_{j-1} - 2y_j), \\ \dot{y}_j &= rx_j - x_j z_j - y_j + \frac{D^b}{2}(y_{j+1} + y_{j-1} - 2y_j), \\ \dot{z}_j &= x_j y_j - \beta z_j, \quad j = 1, \dots, N. \end{aligned} \quad (2)$$

Parameters σ and b are chosen to be the standard ones, $\sigma = 10$ and $\beta = 8/3$. Depending on the kind of coupling, two different values of the parameter r [15] were selected: (i) $r = 8$ and (ii) $r = 14$. For both cases, the Lorenz oscillator does not exhibit a chaotic attractor [16], but simply a *symmetric* bistable phase space with two stable spiral points $C_{\pm} = (\pm \sqrt{\beta(r-1)}, \pm \sqrt{\beta(r-1)}, r-1)$ and a saddle point located at the origin.

In Eq. (2), D^a and D^b account for the coupling coefficients between cells for the two cases studied here; the off- and on-diagonal coupling, respectively. From now on, since most of the results are independent of the kind of coupling, we will use D both for the off- ($D^a = D, D^b = 0$) and on-diagonal ($D^a = 0, D^b = D$) cases. The dynamical system above was numerically integrated using a fourth order Runge-Kutta method. Free ends were considered for the y variable. As initial condition, half of the oscillators were considered to be in the steady state C_+ , while the rest of cells were located at C_- .

Depending on the coupling strength D , different asymptotic states were obtained, Fig. 1. The transition to the propagating solution is as follows; as the coefficient D is increased the boundary between domains of both solutions (C_+ and C_-) becomes smoother than the steplike boundary observed for $D=0$. That is, some oscillators move to the vicinity of C_+ and C_- . For a given value of D the boundary starts to oscillate, i.e., the front undergoes a Hopf bifurcation, but it does not propagate. Finally, for values of D greater than some threshold D_{th} propagation occurs. Both senses are equally probable because of the symmetry of the system, although in Fig. 1 we show the transition from C_+ to C_- .

*E-mail address: diego@fmmeteo.usc.es; http://chaos.usc.es

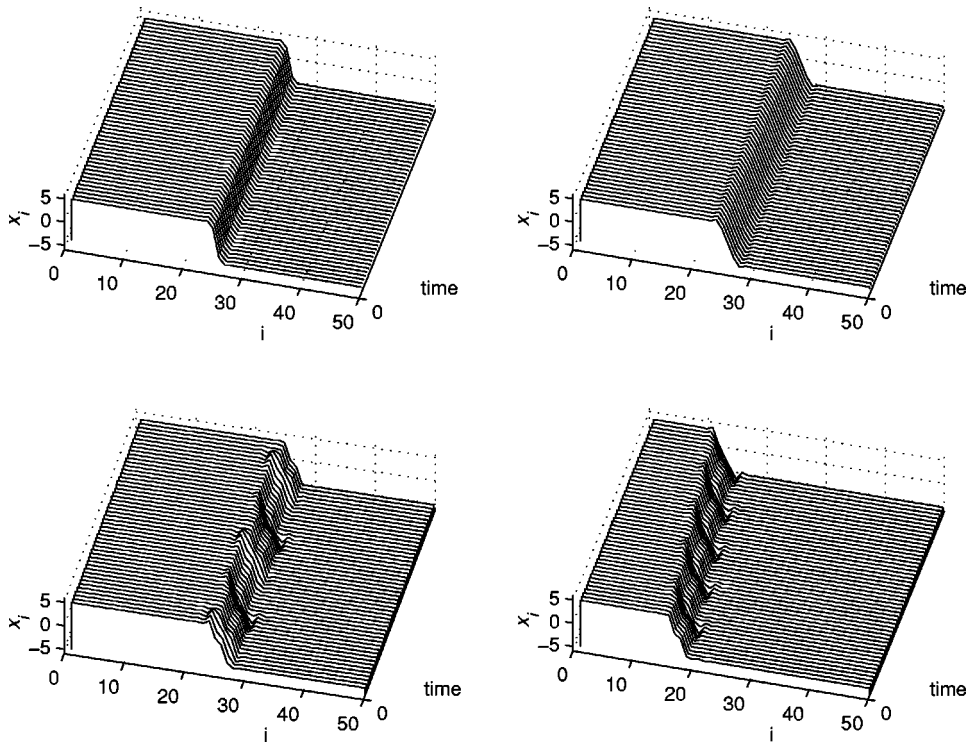


FIG. 1. Spatiotemporal evolution of the wave front as the coupling strength D is increased. A steplike initial condition is imposed for an open array of $N=50$ oscillators: $\mathbf{r}_i \approx C_+$, $i=1, \dots, 25$; $\mathbf{r}_j \approx C_-$, $j=26, \dots, 50$. Depending on the value of D , three different states are achieved. For $D \leq 7.5$ ($D=4$ and $D=7.5$ are shown at the panels above) the system evolves to a standing front, for $D=8.8 < D_{th}$ the front oscillates but still does not propagate, while for $D=8.9 > D_{th}$ the front propagates through the array shifting the oscillators from C_+ to C_- . The time interval shown is 20 time units and the kind of coupling used in this figure was the off-diagonal one.

For a finite open array (null-flow boundary condition), the whole system collapses finally to one of the two stable solutions. On the other hand, for the case of a ring (periodic boundary condition), stationary wave-front solutions can be found. Note as well that for values of D greater than the threshold value D_{th} , the front oscillates with some frequency, which increases with the coupling strength.

Each regime (oscillating or propagating) is characterized by an intrinsic quantity. We measured the period of oscillation (T_1) for the oscillating regime, and the speed of the front (c) for the propagating one. Some special features at both sides of the critical point D_{th} were obtained. First of all, the period of oscillation of the front (T_1) diverges as one approaches to D_{th} from below, while for $D > D_{th}$ we obtained a non-standard dependence of the front velocity c with D . The velocity grows from zero abruptly at $D=D_{th}$, but it does not follow the typical square root law dependence with D [17]. The divergence of T_1 and c^{-1} is of logarithmic type in the neighborhood of D_{th} , as it is shown in the left-most graphs of Fig. 2. Two semilog plots of $T_1/2$ and c^{-1} as a function of $|D-D_{th}|$ are shown in the right-hand side of Fig. 2 for both kinds of coupling used in this Rapid Communication. The meaning of the slope for both curves ($-\lambda_u^{-1}$) is explained below. It is remarkable that $T_1/2$ and c^{-1} behave quite similarly under $|D-D_{th}|$ for a large interval of values, and for both, off- and on-diagonal couplings. On the other hand, for larger values of r (e.g., $r \sim 20$), the transition becomes more convoluted for both types of coupling studied here. The front displays *spontaneous* reversals just above D_{th} , which makes it difficult to measure the front velocity with high precision. Nonetheless, far enough from the transition (in absence of front reversals), one observes that $T_1/2$ and $1/c$ decay with $\ln(|D-D_{th}|)$ and both curves follow similar functions within a 20% of tolerance.

To better describe the transition to front propagation once the Hopf bifurcation occurs, instead of considering the array as a dynamical system with many degrees of freedom, it is worthwhile to describe the transition to propagation in a reduced phase space with coordinates,

$$\xi = \frac{1}{\sqrt{2}} \sum_{j=1}^N x_j + y_j \quad \text{mod}(2\sqrt{2\beta(r-1)}), \quad (3)$$

$$\eta = \frac{1}{\sqrt{2}} \sum_{j=1}^N -x_j + y_j, \quad (4)$$

with the coordinate ξ defined cyclic. The movement of the front shifts a cell from C_{\pm} to C_{\mp} so the system returns to a state dynamically equivalent. In our case, as the front moves to a new cell, the value of ξ increases or decreases an amount $\Delta\xi = 1/\sqrt{2}(2\sqrt{\beta(r-1)} + 2\sqrt{\beta(r-1)}) = 2\sqrt{2\beta(r-1)}$, which is the range where ξ must be defined.

Figure 3 shows the evolution of the front in the cylindrical phase space determined by ξ and η . For D larger than some critical value, the system undergoes a supercritical Hopf bifurcation, so the front starts to oscillate around the steady state $\xi = \eta = 0$. The cycle grows as D is increased and for a critical point D_{th} the orbit transforms into two homoclinic loops. The situation is quite similar to a pendulum with the critical energy for its dynamics to go along one of the two separatrices that isolate libration from rotation. In our case libration corresponds to the oscillation of the front, while rotation corresponds to front propagation. We can characterize our phase space, near the threshold, with the equivalent phase space [18] illustrated schematically in Fig. 4. The bifurcation consists in a gluing (resp. splitting) of two (resp.

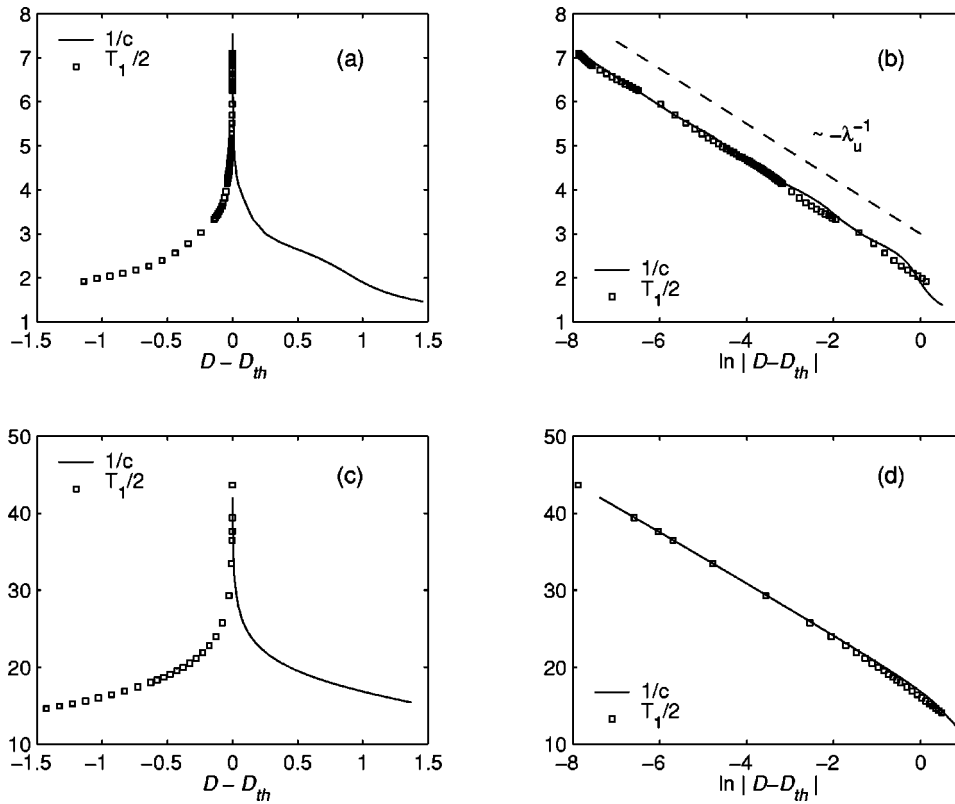


FIG. 2. $1/c$ (solid line) and $T_1/2$ (squares) as a function of $D - D_{th}$ (a), (c) and $\ln |D - D_{th}|$ (b), (d) for the off-diagonal (a), (b) and on-diagonal (c), (d) couplings. The behavior is quite similar, near the onset of the traveling waves, as expected from Eqs. (6) and (7). Both semilog plots may be fitted to a straight line with slope $-\lambda_u^{-1}$ (λ_u is the eigenvalue associated to the unstable eigenvector of the saddle point) as expected from Eqs. (6) and (7). For the off-diagonal coupling (a), (b) $r=8$, $D_{th} \approx 8.841526$ and $\lambda_u^{-1} \approx 0.637$, while for the on-diagonal coupling (c), (d) $r=14$, $D_{th} \approx 39.62838$ and $\lambda_u^{-1} \approx 3.36$.

one) cycles. Analogous *gluing bifurcations* appear in systems with \mathbf{Z}_2 symmetry [19,20], as it happens in our system. Note that Eq. (2) is invariant under the transformation

$$(x_1, y_1, z_1, \dots, x_N, y_N, z_N) \rightarrow (-x_1, -y_1, z_1, \dots, -x_N, -y_N, z_N) \quad (5)$$

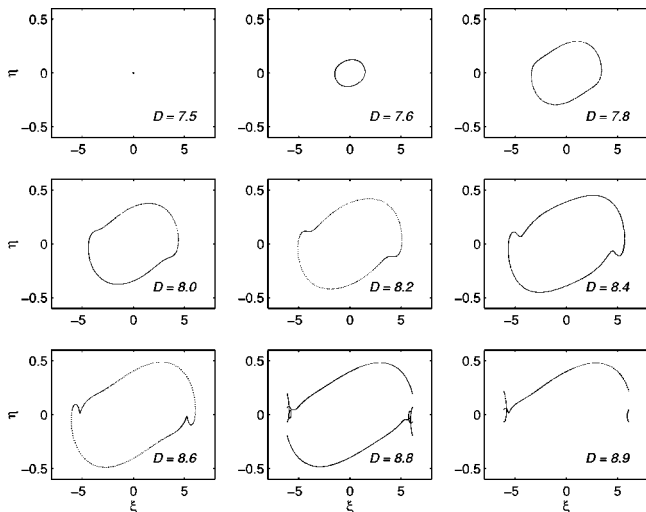


FIG. 3. Evolution of the reduced phase space (ξ, η) as the coupling strength D increases for the off-diagonal case. As D increases, oscillations enlarge their amplitude. Finally, for $D = D_{th} \approx 8.841526$ the orbit collides with itself (in a cylindrical phase space), resulting in two homoclinic connections. Some spurious intersections arise for $D \approx D_{th}$ because of the projection onto a two-dimensional space.

for both couplings.

In 1990, Gaspard [21] obtained the period lengthening of a limit cycle that collides with a hyperbolic fixed point resulting in a homoclinic connection. This scenario is characterized by the logarithmic divergence of the period of the orbit as the threshold value is approached as it was shown in Fig. 2. Then, it is straightforward to extend the analysis to our case (see Fig. 4) where a *double* homoclinic connection appears. The period of the oscillations (T_1) of the front behaves when approaching D_{th} in the following manner,

$$T_1 = a_1 - \frac{2}{\lambda_u} \ln(D_{th} - D), \quad (6)$$

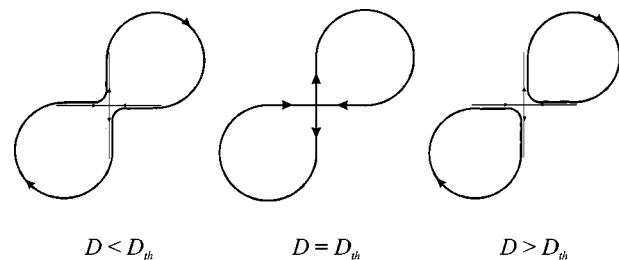


FIG. 4. Schematic of the bifurcation sequence for the double-homoclinic connection in a plane phase portrait. This transition has been previously named *gluing bifurcation* [20]. For $D < D_{th}$ the trajectory approaches twice per cycle to the saddle point and the front oscillates. Beyond D_{th} , the double homoclinic loop splits into two cycles, corresponding to both senses of propagation of the front.

where λ_u is the unstable eigenvalue of the saddle and the factor 2 appears because the orbit crosses twice per cycle close to the saddle point.

On the other hand, for the propagating region the period of oscillation (in the periodic phase space) is the inverse of the velocity (c) of the front. Then,

$$\frac{1}{c} = T_2 = a_2 - \frac{1}{\lambda_u} \ln(D - D_{th}). \quad (7)$$

Therefore, close to the threshold both magnitudes $T_1/2$ and $1/c$ should exhibit the same dependence with $\ln(|D - D_{th}|)$. Moreover, it must be noted that close to the onset the fast dynamics (i.e., far from the saddle point) will be quite similar in the propagating region and in the oscillating one. Thus, it is expected that $a_1 \approx 2a_2$. This last reasoning and the logarithmic dependence on $|D - D_{th}|$ predicted by Eqs. (6) and (7) are successfully confirmed by Fig. 2 for both types of coupling studied in this paper. Even for larger values of r where some discrepancies were found between $T_1/2$ and $1/c$ as a function of the logarithmic coupling strength, the differences were smaller enough to consider that the main underlying mechanism continues to be the one explained above, although in a more complex way. Thus, for high values of r the homoclinic connection is of saddle-focus type (the stable eigenvalues are complex conjugates, $\lambda_s = \rho \pm i\omega$). This would not be important regarding the phenomena discussed in this paper unless the Shil'nikov condition is fulfilled (λ_u

$> -\rho > 0$) [22]. In this case (see Ref. [19]), a more complex scenario develops (including homoclinic chaos that originates spontaneous reversals of the front) [23].

Which are all the necessary ingredients to find the bifurcation route explained here is still a matter of future research. Nonetheless, some conditions must be fulfilled: multivariable nongradient units and a coupling preserving global Z_2 symmetry.

Finally, it must be noted that previous studies [7,9] that take the value of the coupling strength up to which all the stationary solutions of the array continue to exist, as a lower bound for wave propagation, are not suitable for the scenario explained here.

In conclusion, a route to front propagation in arrays of bistable systems has been presented. The dependence of the velocity of the front with the coupling strength is explained by the occurrence of a double homoclinic connection which is found for different couplings [24]. The logarithmic vanishing of the front velocity with D is different of the standard root square dependence, found in multitude of systems.

Some phenomena, for example the short wavelength bifurcation [25], do not have the trivial continuum limit. This is the case of our transition that must be considered a genuine effect of discreteness.

The support by DGES and MCyT under Research Grant Nos. PB97-0540 and BFM2000-0348 is gratefully acknowledged.

-
- [1] M.C. Cross and P.C. Hohenberg, *Rev. Mod. Phys.*, **65** 851 (1993); C. Bowman and A.C. Newell, *ibid.*, **70**, 289 (1998).
- [2] *Optical Bistability*, edited by C. M. Bowden, M. Cifan, and J. R. Robl (Plenum, New York, 1981).
- [3] J.P. Laplante and T. Erneux, *J. Phys. Chem.* **96**, 4931 (1992).
- [4] J.D. Murray, *Mathematical Biology* (Springer-Verlag, New York, 1993).
- [5] H.P. McKean, *Adv. Math.* **4**, 209 (1970).
- [6] R. FitzHugh, *Biophys. J.* **1**, 445 (1961).
- [7] J.P. Keener, *SIAM (Soc. Ind. Appl. Math.) J. Appl. Math.* **47**, 556 (1987); T. Erneux and G. Nicolis, *Physica D* **67**, 237 (1993).
- [8] V. Pérez-Muñozuri, V. Pérez-Villar, and L.O. Chua, *Int. J. Bifurcation Chaos Appl. Sci. Eng.* **2**, 403 (1992); A.P. Muñozuri, V. Pérez-Muñozuri, M. Gómez-Gesteira, L.O. Chua, and V. Pérez-Villar, *ibid.* **5**, 17 (1995).
- [9] R.S. MacKay and J.-A. Sepulchre, *Physica D* **82**, 243 (1995).
- [10] K. Kladko, I. Mitkov, and A.R. Bishop, *Phys. Rev. Lett.* **84**, 4505 (2000); A. Carpio and L.L. Bonilla, *ibid.* **86**, 6034 (2001).
- [11] A. Hagberg and E. Meron, *Nonlinearity* **7**, 805 (1994).
- [12] B. Ziner, *SIAM (Soc. Ind. Appl. Math.) J. Math. Anal.* **22**, 1016 (1991).
- [13] G. Fáth, *Physica D* **116**, 176 (1998).
- [14] E.N. Lorenz, *J. Atmos. Sci.* **20**, 130 (1963); H. Haken, *Phys. Lett. A* **53**, 71 (1975).
- [15] For each case propagation succeeded for $r > 4$ and $r > 13$, respectively.
- [16] C. Sparrow, *The Lorenz Equations: Bifurcations, Chaos and Strange Attractors* (Springer-Verlag, New York, 1982).
- [17] D. Pazó, N. Montejo, and V. Pérez-Muñozuri, *Phys. Rev. E* **63**, 066206 (2001).
- [18] From a topological point of view, the operations we performed to transform a cylinder into a plane are the following. First of all, cut the cylinder with two planes perpendicular to its axis in such a way that the saddle point and the homoclinic orbits stay between both planes. Then, compress the circumferences that limit the "cylinder" to a point. In this moment our object is topologically equivalent to a sphere. After this, make a hole at $\xi = \eta = 0$. Finally, deform what remains into a plane.
- [19] P. Glendinning, *Phys. Lett. A* **103**, 163 (1984).
- [20] J.M. Lopez and F. Marques, *Phys. Rev. Lett.* **85**, 972 (2000).
- [21] P. Gaspard, *J. Phys. Chem.* **94**, 1 (1990).
- [22] J. Guckenheimer and P. Holmes, *Nonlinear Oscillations, Dynamical Systems, and Bifurcations of Vector Fields* (Springer-Verlag, New York, 1983); Y.A. Kuznetsov, *Elements of Applied Bifurcation Theory* (Springer-Verlag, New York, 1995).
- [23] D. Pazó *et al.* (unpublished).
- [24] Another case that shows wave propagation corresponds to the off-diagonal coupling ($\Gamma = \gamma_{kl} = \delta_{k2} \delta_{l1}$), which is equivalent to the one shown in this Rapid Communication.
- [25] J.F. Heagy, L.M. Pecora, and T.L. Carroll, *Phys. Rev. Lett.* **74**, 4185 (1995).